

# Numerical Prediction of Bearing Strength on Composite Bolted Joint Using Three Dimensional Puck Failure Criteria

M. S. Meon, M. N. Rao, K-U. Schröder

**Abstract**—Mechanical fasteners especially bolting is commonly used in joining carbon-fiber reinforced polymer (CFRP) composite structures due to their good joinability and easy for maintenance characteristics. Since this approach involves with notching, a proper progressive damage model (PDM) need to be implemented and verified to capture existence of damages in the structure. A three dimensional (3D) failure criteria of Puck is established to predict the ultimate bearing failure of such joint. The failure criteria incorporated with degradation scheme are coded based on user subroutine executed in Abaqus. Single lap joint (SLJ) of composite bolted joint is used as target configuration. The results revealed that the PDM adopted here could sufficiently predict the behaviour of composite bolted joint up to ultimate bearing failure. In addition, mesh refinement near holes increased the accuracy of predicted strength as well as computational effort.

**Keywords**—Bearing strength, bolted joint, degradation scheme, progressive damage model.

## I. INTRODUCTION

THE extensive use of laminated composite especially for CFRP in aerospace and automotive applications over the years indicates the importance of this material to the world. Their excellent qualities such as high specific strength, fatigue and corrosion resistance as well as the stiffness-to-weight ratio are fascinating characteristics mainly for light weight structures. The use of CFRP laminated structures fastened by bolting connections is quite common in many structures. However, notches manufactured for this connections produced severe stress concentrations [1]. The areas near the holes experience higher stress concentration factors compared to areas further away from this region. This situation tends to create damage initiation leading to total failure of the corresponding structure. Thus, the PDM is frequently used to make prediction of failure in composite structures.

The initial works related to predicting the damage on composite structures started in decades and many damage modelling approaches are presented and discussed in thorough investigations. Until now, there are four damage modelling techniques in composites referred as failure criteria, fracture mechanics, plasticity and damage mechanics approaches [2]. Among those methods, failure criteria is mostly used by many researchers to predict damage on composite structures. The criteria is usually formulated based on stresses and performed well when compared to experimental results [3].

The idea of implementing PDM to composite structures numerically is presented in the detailed explanation highlight the use of failure criteria and degradation techniques [4], [5]. The pioneering works on predicting failure of unidirectional (UD) composite structures based on different type of failure modes are presented by Hashin and Rotem [6], [7] where the theory used is able to identify four major failure modes namely tensile and compressive fibre and matrix failures. Yamada and Sun [8] proposed a failure theory based on the in-situ strength that suited for the fiber controlled laminates. Chang and Chang [9] conducted a more detailed investigation based on Yamada theory by introducing shear nonlinearity mode of failure. A physically based model is developed by Puck and Schürmann [10], which is an extension of Hashin failure criteria emphasising on the fracture angle on the fracture plane. Fracture angle is iteratively evaluated to identify inter-fiber failure (IFF) of any particular structure.

To determine the holistic failure behaviour, failure criteria together with material degradation model are necessary. The most popular degradation scheme is ply discounting (PD) method due to its simple formulation and ease to implement numerically. The degradation technique is achieved either by instantaneous unloading [11], gradual unloading [12] or constant stress [13] at ply failure. Once failure is initiated or detected, stiffness parameters are reduced based on corresponding failure modes. Conducting failure assessment of bolted joints incorporating PDMs becoming a field of interest since the existence of finite element (FE) approach. The factors influencing the damage behaviour of bolted joint include material properties [14], coefficient of friction [15], [16], bolt shape [17], [18] and clearance [19]. Camanho and Matthews [20] analysed the progression and strength of mechanically fastened joints in composite laminates using 3D failure criteria of Hashin with stiffness degradation approach. Ireman [21] conducted a wide range of experiments related to bolted joint of composite and aluminium structures, as well as stress analysis numerically. McCarthy et. al [19] focussed on variation bolt-hole clearance and its effect on the total strength. Hashin 3D model is used with simple sudden degradation technique. Analysis of bearing failure on bolted joints is performed by Riccio [18] by including the effect of fibre-matrix shear out failure in 3D Hashin theory to make the evaluation more meaningful. Effect of delamination is studied in Tserpes et. al [22] works concerning prediction of residual strength and ultimate failure of single-lap bolted joint. The model mentioned above gave good approximation with

M. S. Meon, M. N. Rao and K-U. Schröder (professor) are with Institute of Structural Mechanics and Lightweight Design, RWTH Aachen University, 52062 Aachen, Germany (e-mail: suhairil.meon@sla.rwth-aachen.de, rao.mekala@sla.rwth-aachen.de, kai-uwe.schroeder@sla.rwth-aachen.de).

experimental data.

Based on previous studies, the strength analysis in 3D failure criteria of Puck combined with ply discount method for bolted joints are performed in this paper. 3D failure theory is crucially needed in order to capture damage initiation, especially for joined structures. As motivation to develop such a simple and reasonable damage model suited for composite structures, combination of maximum stress failure theory and Puck's formulation is seen to numerically compute the failure in proper manner. The PDM is developed using Fortran code and linked to Abaqus for numerical evaluation. The numerical results are verified by experimental data available from literature.

## II. PROGRESSIVE DAMAGE MODEL

Progressive damage model consists of damage initiation and progression criterion. Damage initiation is detected through the use of failure criteria for fibre failure (FF) and inter-fibre failure (IFF). Damage evolution approach is used to analyse propagation of damage by degrading the material properties (i.e reduced stiffness matrix).

### A. Physically Based Failure Criteria

A three-dimensional failure theory of Puck [10] is used in this paper to predict the failure initiation of composite joint. The failure criteria is divided into two major mode of failures which are fibre failure (FF) and inter-fibre failure (IFF), both in tension and compression. for the sake of simplification, FF is evaluated based on maximum stress failure theory (MSFT) and written as:

$$FF = \begin{cases} \frac{\sigma_1}{X_T} & \text{for } \sigma_1 > 0 \\ \frac{\sigma_1}{-X_C} & \text{for } \sigma_1 < 0 \end{cases} \quad (1)$$

where  $X_T$  and  $X_C$  are the longitudinal tensile and compressive strength, respectively. The stresses acting on the fracture plane is assumed to create the fracture and contributed to the inter-fibre failure (IFF). The fracture plane is arbitrary from  $-90^\circ$  to  $+90^\circ$  (symmetry plane) about material plane. A set of transformation equations is needed to obtain normal and shear stresses acting on the action plane.

$$\sigma_n(\theta) = \sigma_2 \cos^2(\theta) + \sigma_3 \sin^2(\theta) + 2\tau_{23} \sin(\theta) \cos(\theta) \quad (2)$$

$$\tau_{nt}(\theta) = (\sigma_3 - \sigma_2) \sin(\theta) \cos(\theta) + \tau_{23}(\cos^2(\theta) - \sin^2(\theta)) \quad (3)$$

$$\tau_{nl}(\theta) = \tau_{31} \sin(\theta) + \tau_{21} \cos(\theta) \quad (4)$$

The IFF functions can be written as:

$$A = \left[ \left( \frac{1}{R_{\perp}} - \frac{P_{\perp\psi}^+}{R_{\perp\psi}} \right) \sigma_n(\theta) \right]^2 + \left( \frac{\tau_{nt}(\theta)}{R_{\perp\perp}} \right)^2 + \left( \frac{\tau_{nl}(\theta)}{R_{\perp\parallel}} \right)^2 \quad (5)$$

$$B = \left( \frac{\tau_{nt}(\theta)}{R_{\perp\perp}} \right)^2 + \left( \frac{\tau_{nl}(\theta)}{R_{\perp\parallel}} \right)^2 + \left[ \left( \frac{P_{\perp\psi}^-}{R_{\perp\psi}} \sigma_n(\theta) \right) \right]^2 \quad (6)$$

$$IFF = \begin{cases} \sqrt{A} + \frac{P_{\perp\psi}^+}{R_{\perp\psi}} \sigma_n(\theta) & \text{for } \sigma_n \geq 0 \\ \sqrt{B} + \frac{P_{\perp\psi}^-}{R_{\perp\psi}} \sigma_n(\theta) & \text{for } \sigma_n < 0 \end{cases} \quad (7)$$

The parameter  $\psi$  denotes the shear angle in action plane, whilst  $P_{\perp\psi}^+$  and  $P_{\perp\psi}^-$  are the slope parameters represent internal friction effects in Mohr-Coulomb failure criteria. Notation  $R_{\perp}$  indicates failure resistance normal to fibres direction, while  $R_{\perp\psi}$ ,  $R_{\perp\perp}$  and  $R_{\perp\parallel}$  are the fracture resistances of the action plane due to the shear stressing. For the sake of completeness of supplementary equation required for IFF, publication [10] is referred.

### B. Degradation Model and Damage Evolution

Traditionally, elastic stiffness parameters are reduced when failure is initiated. Material properties are reduced either instantaneously (sudden) or gradually (i.e exponential) over certain increments. However, in this analysis, material stiffness matrix itself is reduced instead of components inside the matrix to avoid numerical convergence problems [11]. The constitutive stress-strain relationship with the damage parameters for a 3D orthotropic material can be written as:

$$\begin{Bmatrix} \sigma_{11} \\ \sigma_{22} \\ \sigma_{33} \\ \sigma_{12} \\ \sigma_{13} \\ \sigma_{23} \end{Bmatrix} = \begin{bmatrix} C_{11} & C_{12} & C_{13} & 0 & 0 & 0 \\ C_{21} & C_{22} & C_{23} & 0 & 0 & 0 \\ C_{31} & C_{32} & C_{33} & 0 & 0 & 0 \\ 0 & 0 & 0 & G_{12} & 0 & 0 \\ 0 & 0 & 0 & 0 & G_{13} & 0 \\ 0 & 0 & 0 & 0 & 0 & G_{23} \end{bmatrix} \begin{Bmatrix} \sigma_{11} \\ \sigma_{22} \\ \sigma_{33} \\ \sigma_{12} \\ \sigma_{13} \\ \sigma_{23} \end{Bmatrix} \quad (8)$$

The global damage parameters are successfully coupled with damaged stiffness matrix, and this concept is implemented in Lee et al. [25].

$$d_f = 1 - (1 - d_{ft})(1 - d_{fc}) \quad (9)$$

$$d_m = 1 - (1 - d_{mt})(1 - d_{mc}) \quad (10)$$

$$C_{11} = (1 - d_f) C'_{11} \quad (11)$$

$$C_{12} = (1 - d_f)(1 - d_m) C'_{12} \quad (12)$$

$$C_{13} = (1 - d_f)(1 - d_m) C'_{13} \quad (13)$$

$$C_{22} = (1 - d_f)(1 - d_m) C'_{22} \quad (14)$$

$$C_{23} = (1 - d_f)(1 - d_m) C'_{23} \quad (15)$$

$$C_{33} = (1 - d_f)(1 - d_m) C'_{33} \quad (16)$$

$$G_{12} = (1 - d_f)(1 - s_{mt}d_{mt})(1 - s_{mc}d_{mc}) G'_{12} \quad (17)$$

$$G_{13} = (1 - d_f)(1 - s_{mt}d_{mt})(1 - s_{mc}d_{mc}) G'_{13} \quad (18)$$

$$G_{23} = (1 - d_f)(1 - s_{mt}d_{mt})(1 - s_{mc}d_{mc}) G'_{23} \quad (19)$$

where  $C_{ij}$  and  $C'_{ij}$  are the original and damaged material stiffness tensors, respectively;  $d_{ft}$ ,  $d_{fc}$ ,  $d_{mt}$ ,  $d_{mc}$  are the fibre and matrix degradation factors based on tensile and compressive stress states, respectively. IFF interaction causes the loss control factors  $s_{mt}$  and  $s_{mc}$  for shear stiffness. The

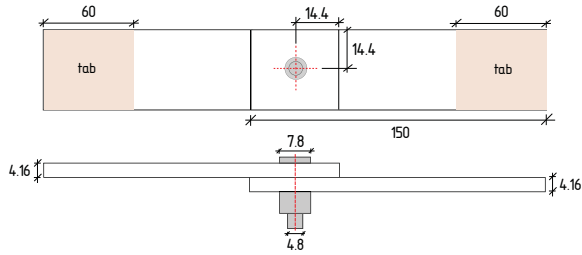


Fig. 1 Geometry of single lap joint according to Riccio's work [18]. All units in mm

TABLE I  
MECHANICAL PROPERTIES OF CFRP COMPOSITE HTA7/6376 [18]

Properties	Value
Longitudinal modulus, $E_1$ (GPa)	145
Transverse modulus, $E_2$ (GPa)	10.3
Transverse modulus, $E_3$ (GPa)	11.1
In-plane shear modulus, $G_{12}$ (GPa)	5.3
Out-of-plane shear modulus, $G_{13}$ (GPa)	5.27
Out-of-plane shear modulus, $G_{23}$ (GPa)	3.95
Major Poisson's ratio, $\nu_{12}$	0.3
Through thickness Poisson's ratio, $\nu_{13}$	0.5
Through thickness Poisson's ratio, $\nu_{23}$	0.5
Longitudinal tensile strength, $X_T$ (MPa)	2250
Longitudinal compressive strength, $X_C$ (MPa)	1600
Transverse tensile strength, $Y_T$ (MPa)	64
Transverse compressive strength, $Y_C$ (MPa)	290
In-plane shear strength, $S_{12}$ (MPa)	120
In-plane shear strength, $S_{13}$ (MPa)	120
Out-of-plane shear strength, $S_{23}$ (MPa)	50

value recommended by Abaqus are 0.9 and 0.5 for  $s_{mt}$  and  $s_{mc}$  respectively. In this publication, an exponential function to represent the internal damage variable is used as shown in equation below. The function is selected based on successful attempt made by Tserpes et al. [22] and other researchers.

$$d_i = 1 - \exp\left[\frac{1}{m}(1 - f_i^m)\right] \quad (20)$$

where subscript  $i$  represents internal damage notation ( $ft, fc, mt, mc$ ) and  $m$  is Weibull's parameter.

### III. NUMERICAL MODEL

A FE model is developed for CFRP bolted joint accordance on geometry and testing setting from Riccio [18]. Riccio conducted failure analysis of his experimental results by adopting 3D Hashin failure criteria. Later, Santiuste and Olmedo [15] replicated similar setting together with Chang-Lessard criteria.

A single lap joint (SLJ) is fabricated by using HTA7/6376 CFRP composite laminates and aerospace grade Ti-6Al-4V STA bolt and nut. The stacking sequence for the laminated composite plate is  $[(0/\pm 45/90)_4]_s$ . The geometry of SLJ and properties of material used can be found in Fig. 1, Tables I and II, respectively. The joint is fixed at one end and allowed to move in the direction of applied load for the other side of joint.

TABLE II  
ELASTO-PLASTIC PROPERTIES OF Ti-6AL-4V STA

Young's modulus, $E$ (MPa)	Poisson's ratio (-)
110000	0.29
True stress (MPa)	True plastic strain (-)
950	0.0
1034	0.002
1103	0.1

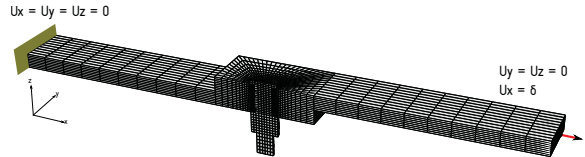


Fig. 2 FE mesh, boundary conditions and loading direction (cross-sectional view)

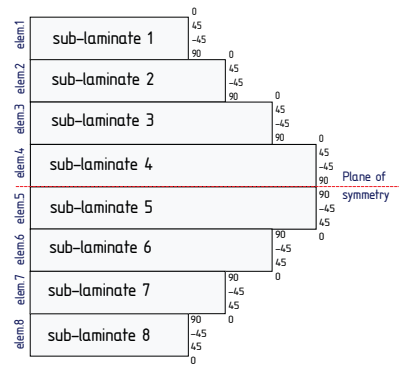


Fig. 3 Layer configuration for FE calculation based on 8-element through thickness, later referred as sub-laminate

#### A. Modelling SLJ

This exercise is aimed to capture the failure behaviour of composite bolted joint in the case of bearing failure. Brick elements with reduced integration (C3D8R) are used to mesh all part in the joint. Mesh refinement is made especially near holes to capture failure as well as to improve contact mechanism. To reduce the computational effort, eight elements through thickness are partitioned, and each sub-laminate represented as one element per-thickness as illustrated in Fig. 3. Bolt, nut and washer are modelled as single bolt construction to reduce number of degrees of freedom.

Pretensioning is applied to the bolt (tightening effect) using bolt load procedure in Abaqus. A 5-kN bolt load is used to tighten the bolt, and then 2-mm prescribed displacement is provided to the model for translating the joint. In general, evaluating the bearing strength of lap-joint requires two steps;

- 1) Tightening torque is applied to the bolt as a bolt load
- 2) Bolt length has remained fix, and the load is applied longitudinally at the free end of plate

#### B. Contact and Boundary Conditions

Contact interactions are modelled using the surface to surface principle considering the linear penalty method. The normal behaviour is characterized by the 'hard' method, while

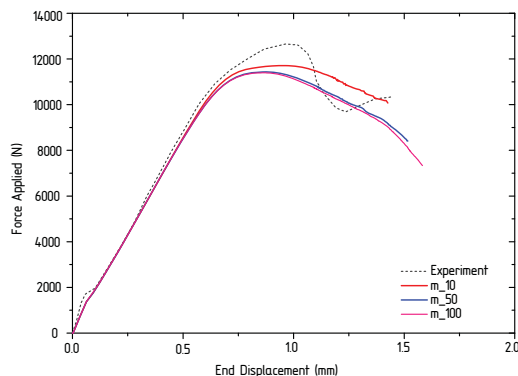


Fig. 4 Load-displacement curve for viscous parameter of 0.03 and variation of Weibull constants

the tangential behaviour is realised using classic Coulomb friction model. As suggested by McCarthy et al. [17], a value of 0.3 is used as friction coefficient for all contacted surfaces.

Five contact interactions are identified and referred as bolt-top plate, top plate-bolt shank, bottom plate-bolt shank, top plate-bottom plate and bottom plate-nut. Since no clearance between bolt shank circumferences and hole. All interactions are placed during initial step.

### C. Viscous Regularisation

Convergence difficulty is the major drawback associated with numerical simulation using implicit platform [23], [24]. Since the model developed here considered strain softening and degradation of material stiffness, often the process terminated earlier due to convergence issues. Thus, a viscous regularisation scheme is used to improve the convergence and implemented through an equation as follows [23]:

$$\dot{d}_i^v = \frac{1}{\eta} (d_i - d_i^v), \quad i = \{ft, fc, mt, mc\} \quad (21)$$

where  $d_i$  and  $d_i^v$  are damage variables defined and regularised damage variable, respectively. The coefficient of viscosity,  $\eta$  is used to control the regularisation scheme.

For the  $(1 + i)$ th increment, the scheme can be written as:

$$d_{i,n+1}^v = \frac{\Delta t}{\eta + \Delta t} d_{i,n+1} + \frac{\eta}{\eta + \Delta t} d_{i,n+1}^v \quad (22)$$

## IV. RESULT AND DISCUSSION

### A. Model Validation

The FE results generated by developed PDM are compared to experimental Load-displacement curve provided by Riccio [18]. The aim of this assessment is to predict the ultimate bearing load or to evaluate load bearing capacity. The SLJ lost its load bearing capacity at approximately 12.6-kN as shown in Fig. 4. The proposed PDM exhibited non-linearity of load-displacement curve, as well as while damage is in propagation.

### B. Damage Mechanism

Analysis of damage around the holes is conducted to clarify type of failure modes during failure initiation and progression phases as displayed in Fig. 5. The value of 1.0 represents the total failure and 0.0 for no failure occurs. The results proved that bearing failure contributed to total failure of respective structure.

Fig. 5d clearly indicated that the maximum value of IFF (matrix cracking) are located at the lower plies due to the secondary bending effect. Thus, the distribution of matrix failure is non-uniform throughout the plate's thickness. Moreover, tightening torque which applied at the beginning of analysis also increased the matrix failure as can be seen at the top of composite plate in Fig. 5c.

At the onset of ultimate failure, fibre failure (FF) due to compressive load is identified, and caused by movement of bolt's shank towards the surface of composite plates as shown in Fig. 5b. The bottom part of the plate experienced failure first followed by top surface.

### C. Effect of Weibull's Constants, $m$

A parametric study is carried out to investigate the effect of changing Weibull's constant  $m$  on the ultimate bearing load. In this case, viscous regularisation parameter is remained constant as 0.03. The results in Fig. 4 indicated that the constants  $m$  used here are significantly affected on the slope of degradation and not on the value of maximum failure load. Increasing value of  $m$  lead to decrease the degradation's slope.

### D. Effect of Viscous Regularisation Parameter

Fig. 6 shows the load-displacement curve for different value of viscous parameter, while  $m = 100$  is maintained as degradation constant. Increasing the viscous parameter from 0.009 to 0.05 yields to higher the magnitude of ultimate failure load. This parameter setting helped to reduce the problem related to convergence solution.

### E. Effect of Lay-up Technique

In order to examine the effect of modelling the plies, two type of lay-up models are considered; 8-element (sub-laminate, as in Fig. 3) and 32-element (layer-wise (LW)) throughout thickness of composite plate. The selection of sub-laminate strategy is based on work of Riccio [18], however modification is made according to McCarthy et al. [17].

It can be concluded from Fig. 7 that sub-laminate approach performed better in predicting the ultimate bearing load as compared with LW approach. The LW model experienced convergence issue and high computing time consumption. Even though LW in this study less accurate, damage accumulation trend is more feasible when compare to experimental curve. In general, both approaches under-predicted the maximum bearing load obtained from experiment.



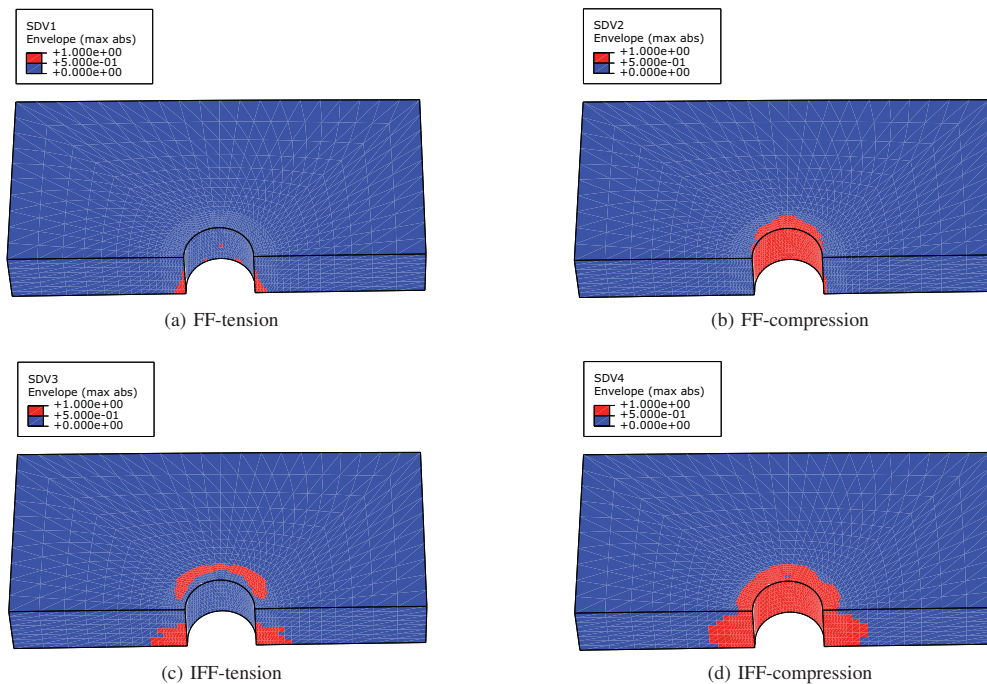


Fig. 5 Cross-section of composite plate at 12.6 kN and the corresponding damage variables (top plate, half view)

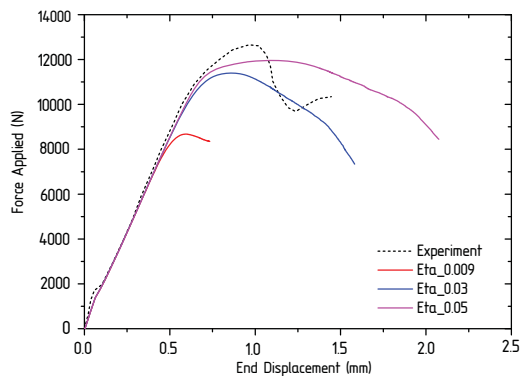


Fig. 6 Load-displacement curve for fixed value of Weibull constant of 100, and different values of viscous parameter

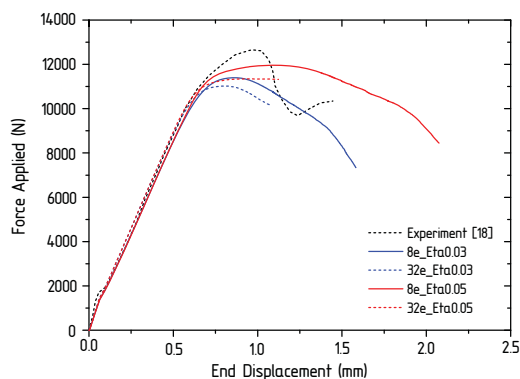


Fig. 7 Load-displacement curve for fixed value of Weibull constant of 100 and different values of viscous parameter, as well as through thickness meshing approach

## V. CONCLUSION

In this paper, a progressive damage model of single-lap, single protruded bolt composite joint is established. The present failure criteria pointed out the utilisation of maximum stress theory to predict fibre breakage and Puck's formulation to evaluate inter-fibre failure or matrix cracking. A 3D failure criteria is necessary to predict damage accumulation in the case of lap-joint in composite structures. Numerical model developed here mimicked similar set-up with experiment conducted by Riccio [18] except for clearance between shank and holes. The model includes the tightening torque and also reasonable friction coefficient to represent contact behaviour between bolt and composite plates especially at the vicinity of the holes. The secondary bending and pre-tension of bolt, as well as artificial viscous parameter selected influenced the accuracy of PDM used. The numerical results proved successfully that the model developed is highly capable in assessing the damage behaviour of single lap composite bolted joint.

## ACKNOWLEDGMENT

The authors would gratefully acknowledge the financial support from the Ministry of Higher Education (MOHE), Malaysia for the first author.

## REFERENCES

- [1] Y. Liu, B. Zwingmann, and M. Schlaich, "Nonlinear progressive damage analysis of notched or bolted fibre-reinforced polymer (FRP) laminates based on a three-dimensional strain failure criterion," *Polymers*, vol. 6, no. 4, pp. 949–976, 2014.

- [2] M. V. Donadon, S. F. M. De Almeida, M. A. Arbelo, and A. R. de Faria, "A three-dimensional ply failure model for composite structures," *International Journal of Aerospace Engineering*, vol. 2009, 2009.
- [3] K. Rohwer, "Predicting fibre composite damage and failure," *Journal of Composite Materials*, vol. 49, no. 21, pp. 2673–2683, 2015.
- [4] O. O. Ochoa and J. N. Reddy, *Finite Element Analysis of Composite Laminates*. Dordrecht: Springer Netherlands, 1992, ch. Finite Element Analysis of Composite Laminates, pp. 37–109.
- [5] N. F. Knight Jr and J. R. Reeder, "User-defined material model for progressive failure analysis," 2006.
- [6] Z. Hashin and A. Rotem, "A fatigue failure criterion for fiber reinforced materials," *Journal of Composite Materials*, vol. 7, no. 4, pp. 448–464, 1973.
- [7] Z. Hashin, "Failure criteria for unidirectional fiber composites," *Journal of Applied Mechanics*, vol. 47, no. 2, pp. 329–334, 1980.
- [8] S. Yamada and C. Sun, "Analysis of laminate strength and its distribution," *Journal of Composite Materials*, vol. 12, no. 3, pp. 275–284, 1978.
- [9] F.-K. Chang and K.-Y. Chang, "A progressive damage model for laminated composites containing stress concentrations," *Journal of Composite Materials*, vol. 21, no. 9, pp. 834–855, 1987.
- [10] A. Puck and H. Schrmann, "Failure analysis of FRP laminates by means of physically based phenomenological models," *Composites Science and Technology*, vol. 58, no. 7, pp. 1045–1067, 1998.
- [11] S. Arunkumar and A. Przekop, "Predicting failure progression and failure loads in composite open-hole tension coupons," 2010.
- [12] L. Zhao, T. Qin, J. Zhang, and Y. Chen, "3D gradual material degradation model for progressive damage analyses of unidirectional composite materials," *Mathematical Problems in Engineering*, vol. 2015, p. 11, 2015.
- [13] H. Hahn and S. Tsai, "On the behavior of composite laminates after initial failures," *Journal of Composite Materials*, vol. 8, no. 3, pp. 288–305, 1974.
- [14] Y. Xiao and T. Ishikawa, "Bearing strength and failure behavior of bolted composite joints (part ii: modeling and simulation)," *Composites Science and Technology*, vol. 65, no. 7-8, pp. 1032–1043, 2005.
- [15] I. Olmedo and C. Santiuste, "On the prediction of bolted single-lap composite joints," *Composite Structures*, vol. 94, no. 6, pp. 2110–2117, 2012.
- [16] W.-H. Chen, S.-S. Lee, and J.-T. Yeh, "Three-dimensional contact stress analysis of a composite laminate with bolted joint," *Composite Structures*, vol. 30, no. 3, pp. 287–297, 1995.
- [17] M. A. McCarthy, C. T. McCarthy, V. P. Lawlor, and W. F. Stanley, "Three-dimensional finite element analysis of single-bolt, single-lap composite bolted joints: part i model development and validation," *Composite Structures*, vol. 71, no. 2, pp. 140–158, 2005.
- [18] A. Riccio, "Effects of geometrical and material features on damage onset and propagation in single-lap bolted composite joints under tensile load: part ii numerical studies," *Journal of Composite Materials*, vol. 39, no. 23, pp. 2091–2112, 2005.
- [19] M. A. McCarthy, V. P. Lawlor, W. F. Stanley, and C. T. McCarthy, "Bolt-hole clearance effects and strength criteria in single-bolt, single-lap, composite bolted joints," *Composites Science and Technology*, vol. 62, no. 1011, pp. 1415–1431, 2002.
- [20] P. Camanho and F. Matthews, "A progressive damage model for mechanically fastened joints in composite laminates," *Journal of Composite Materials*, vol. 33, no. 24, pp. 2248–2280, 1999.
- [21] T. Ireman, "Three-dimensional stress analysis of bolted single-lap composite joints," *Composite Structures*, vol. 43, no. 3, pp. 195–216, 1998.
- [22] K. I. Tserpes, P. Papanikos, and T. H. Kermanidis, "A three-dimensional progressive damage model for bolted joints in composite laminates subjected to tensile loading," *Fatigue & Fracture of Engineering Materials & Structures*, vol. 24, no. 10, pp. 663–675, 2001.
- [23] I. Lapczyk and J. A. Hurtado, "Progressive damage modeling in fiber-reinforced materials," *Composites Part A: Applied Science and Manufacturing*, vol. 38, no. 11, pp. 2333–2341, 2007.
- [24] J. F. Chen, E. V. Morozov, and K. Shankar, "A combined elastoplastic damage model for progressive failure analysis of composite materials and structures," *Composite Structures*, vol. 94, no. 12, pp. 3478–3489, 2012.
- [25] C.-S. Lee, J.-H. Kim, S.-k. Kim, D.-M. Ryu, J.-M. Lee, Initial and progressive failure analyses for composite laminates using puck failure criterion and damage-coupled finite element method, *Composite Structures* 121 (0) (2015) 406–419.